Published online 29 November 2018

Nucleic Acids Research, 2019, Vol. 47, No. 2 **843–854**
doi: 10.1093/nar/gky1201

Regulation of (p)ppGpp hydrolysis by a conserved archetypal regulatory domain

Séverin Ronneau[1], Julien Caballero-Montes[2], Jérôme Coppine[1], Aurélie Mayard[1], Abel Garcia-Pino[2] and Régis Hallez[1,*]

[1]Bacterial Cell cycle & Development (BCcD), Biology of Microorganisms Research Unit (URBM), Namur Research Institute for Life Science (NARILIS), University of Namur, 61 Rue de Bruxelles, 5000 Namur, Belgium and [2]Cellular and Molecular Microbiology, Université Libre de Bruxelles (ULB), 12 Rue des Professeurs Jeener et Brachet, B-6041 Gosselies, Belgium

Received September 15, 2018; Revised November 13, 2018; Editorial Decision November 14, 2018; Accepted November 15, 2018

ABSTRACT

Sensory and regulatory domains allow bacteria to adequately respond to environmental changes. The regulatory ACT (Aspartokinase, Chorismate mutase and TyrA) domains are mainly found in metabolic-related proteins as well as in long (p)ppGpp synthetase/hydrolase enzymes. Here, we investigate the functional role of the ACT domain of SpoT, the only (p)ppGpp synthetase/hydrolase of *Caulobacter crescentus*. We show that SpoT requires the ACT domain to efficiently hydrolyze (p)ppGpp. In addition, our *in vivo* and *in vitro* data show that the phosphorylated version of EIIA^{Ntr} (EIIA^{Ntr}∼P) interacts directly with the ACT and inhibits the hydrolase activity of SpoT. Finally, we highlight the conservation of the ACT-dependent interaction between EIIA^{Ntr}∼P and SpoT/Rel along with the phosphotransferase system (PTS^{Ntr})-dependent regulation of (p)ppGpp accumulation upon nitrogen starvation in *Sinorhizobium meliloti*, a plant-associated α-proteobacterium. Thus, this work suggests that α-proteobacteria might have inherited from a common ancestor, a PTS^{Ntr} dedicated to modulate (p)ppGpp levels in response to nitrogen availability.

INTRODUCTION

Bacteria use a wide range of sensory and regulatory domains to integrate environmental signals. In response to nutrient limitation, most bacteria synthesize a second messenger, the guanosine penta- or tetra-phosphate commonly referred to as (p)ppGpp. This molecule helps in reallocating cellular resources notably by reprogramming transcription and interfering with cell cycle progression (1,2). In *Escherichia coli*, (p)ppGpp levels are regulated by RelA and SpoT, two long RelA/SpoT homologue (RSH) enzymes. SpoT carries a synthetase domain (SD) that is poorly activated by starvation signals (carbon, fatty acids, phosphate, ...) and a functional hydrolase domain (HD). By contrast, RelA harbours an SD activated by amino acid scarcity and a degenerated and inactive HD domain (reviewed in (2) and (3)). Despite these differences, both RSH enzymes present the same domain architecture with catalytic domains (SD and HD) located towards the N-terminus and regulatory domains TGS (ThrRS, GTPase and SpoT) and ACT (Aspartokinase, Chorismate mutase and TyrA) at the C-terminal end (Figure 1). The C-terminal domains (CTD) are thought to play a critical role in RSH by sensing the starvation signal and transducing it to the catalytic domains. RelA, for example, is known to be associated with the ribosome, where it detects deacylated transfer RNA (tRNA) in the ribosomal acceptor site (A-site) as a signal for amino acid starvation, which activates the synthetase activity (4). Recent studies using cryo-electron microscopy revealed that *E. coli* RelA adopts an extended 'open' conformation on stalled ribosomes with the A-site/tRNA in contact with the TGS domain in the C-terminal part (5–7). Likewise, activation of SpoT synthetase activity in *E. coli* cells starved for fatty acids has been shown to require an acyl carrier protein that binds to the TGS of SpoT (8). Although the role of the CTD is undoubtedly critical for regulating catalytic functions of RSH, the mechanisms by which this regulation is mediated remain unknown.

In contrast to *E. coli*, most α-proteobacteria encode bifunctional synthetase/hydrolase RSH usually referred to as Rel or SpoT (9). This is the case of *Caulobacter crescentus,* which harbours a single RSH (SpoT) sensitive to nitrogen or carbon starvation (10,11). *Caulobacter crescentus* divides asymmetrically to generate two dissimilar progeny, a motile swarmer cell and a sessile stalked cell. The stalked cell ini-

*To whom correspondence should be addressed. Tel: +32 81 724 244; Fax: +32 81 724 297; Email: regis.hallez@unamur.be
Present address: Séverin Ronneau, MRC Centre for Molecular Bacteriology and Infection, Flowers Building, Armstrong Road, Imperial College London, London SW7 2AZ, UK.

tiates a new replication cycle (S phase) immediately at birth whereas the swarmer cell first enters into a non-replicative G1 phase before starting replication and concomitantly differentiating into a stalked cell (12). Once accumulated, (p)ppGpp modulates cell cycle progression by specifically extending the G1/swarmer phase (13,14). Recently, we reported a key role played by the nitrogen-related phosphotransferase system (PTS^{Ntr}) in regulating (p)ppGpp accumulation in response to nitrogen starvation (15). We showed that EI^{Ntr}, the first protein of PTS^{Ntr}, uses intracellular glutamine concentration as a proxy for nitrogen availability, since glutamine binds to the GAF domain of EI^{Ntr} to inhibit its autophosphorylation. Therefore, glutamine deprivation strongly stimulates autophosphorylation of EI^{Ntr}, which in turn triggers phosphorylation of the downstream components HPr and $EIIA^{Ntr}$. Once phosphorylated, both HPr∼P and $EIIA^{Ntr}$∼P modulate activities of SpoT to quickly increase (p)ppGpp levels. Whereas HPr∼P stimulates synthetase activity of SpoT by an unknown mechanism, $EIIA^{Ntr}$∼P interacts directly with SpoT to likely interfere with its hydrolase activity (15). The plant-associated α-proteobacterium *Sinorhizobium meliloti* also accumulates (p)ppGpp upon nitrogen or carbon starvation from a single enzyme called Rel (16,17), but the mechanism beyond this regulation remains unknown.

In this work, we investigate the role of the ACT domain in regulating the activity of SpoT-like enzymes. In particular, we show that the ACT is indispensable for the hydrolase activity of *C. crescentus* SpoT and that $EIIA^{Ntr}$∼P inhibits (p)ppGpp hydrolysis likely by directly interacting with the ACT of SpoT. In addition, we show that the $EIIA^{Ntr}$∼P-mediated regulation of RSH is conserved in *S. meliloti*, suggesting PTS^{Ntr} plays a critical role in sensing the metabolic state and regulating cell cycle progression in α-proteobacteria.

MATERIALS AND METHODS

Bacterial strains and growth conditions

Oligonucleotides, strains and plasmids used in this study are listed in Supplementary Tables S1–S3, together with construction details provided in the Supplementary Methods. *E. coli* Top10 was used for cloning purpose, and grown aerobically in Luria-Bertani (LB) broth (Invitrogen) (18). Electrocompetent cells were used for transformation of *E. coli.* All *C. crescentus* strains used in this study are derived from the synchronizable (NA1000) wild-type strain, and were grown in Peptone Yeast Extract (PYE) or synthetic M2 (20 mM PO_4^{3-}, 9.3 mM NH_4^+; +N) or P2 (20 mM PO_4^{3-}; -N) supplemented with 0.5 mM $MgSO_4$, 0.5 mM $CaCl_2$, 0.01 mM $FeSO_4$ and 0.2% glucose (respectively M2G or P2G) media at 28–30°C. Growth was monitored by following the optical density at 660 nm (OD_{660}) during 24 h, in an automated plate reader (Epoch 2, Biotek) with continuous shaking at 30°C. Motility was monitored on PYE swarm (0.3% agar) plates. Area of the swarm colonies were quantified with ImageJ software as described previously (15). For kinetic experiments with *S. meliloti* (Supplementary Figure S5d), bacteria where cultivated overnight at 30°C in LBMC (LB broth with 2.5 mM $MgSO_4$ and 2.5 mM $CaCl_2$) supplemented with kanamycin, then back-diluted in LBMC during 3 h before induction with 0.1 mM isopropyl-β-D-thiogalactoside (IPTG). Samples were taken each hour during 5 h. For *E. coli*, antibiotics were used at the following concentrations (μg/ml; in liquid/solid medium): ampicillin (50/100), kanamycin (30/50), oxytetracycline (12.5/12.5) where appropriate. For *C. crescentus*, media were supplemented with kanamycin (5/20), tetracycline (1/2.5) where appropriate. The doubling time of *Caulobacter* strains was calculated in exponential phase (OD_{660}: 0.2–0.5) using $D = [\ln(2).(T_{(B)} - T_{(A)})) / (\ln(OD_{660(B)})-\ln(OD_{660(A)})]$ and normalized according to the wild-type strain.*E. coli* S17-1 and MT607 helper strains were used for transferring plasmids to *C. crescentus* by respectively bi- and tri-parental mating. In-frame deletions were created by using pNPTS138-derivative plasmids and by following the procedure described previously (15).

Bacterial two-hybrid assays

Bacterial two-hybrid (BTH) assays were performed as described previously in (15). Briefly, 2 μl of MG1655 *cyaA::frt* (RH785) and MG1655 *cyaA::frt* Δ*npr* (RH2122) strains expressing T18 and T25 fusions were spotted on MacConkey Agar Base plates supplemented with ampicillin, kanamycin, maltose (1%), and incubed for 1 day at 30°C. All proteins were fused to T25 (pKT25) or T18 (pUT18C) at their N-terminal extremity. The β-galactosidase assays were performed as described in (15). Briefly, 50 μl *E. coli* BTH strains cultivated overnight at 30°C in LB medium supplemented with kanamycin, ampicillin and IPTG (1 mM) were resuspended in 800 μl of Z buffer (60 mM Na_2HPO_4, 40 mM NaH_2PO_4, 10 mM KCl and 1 mM $MgSO_4$) and lysed with chloroform. After the addition of 200 μl (o-nitrophenyl-β-D-galactopyranoside (ONPG); 4 mg/ml), reactions were incubated at 30°C until colour turned yellowish. Reactions were then stopped by adding 500 μl of 1 M Na_2CO_3, and absorbance at 420 nm was measured. Miller Units are defined as $(OD_{420} \times 1000)/ (OD_{590} \times t \times v)$, where '$OD_{590}$' is the absorbance of the cultures at 590 nm before the β-galactosidase assays, 't' is the time of the reaction (min) and 'v' is the volume of cultures used in the assays (ml). All the experiments were performed with at least three biological replicates.

Flow cytometry analysis

DNA content was measured using Fluorescence-Activated Cell Sorting (FACS) as described previously in (15). Briefly, cells were fixed in ice-cold 70% Ethanol. Fixed samples were then washed twice in FACS staining buffer (10 mM Tris pH 7.2, 1 mM ethylenediaminetetraacetic acid, 50 mM NaCitrate, 0.01% Triton X-100) containing 0.1 mg/ml RNaseA and incubated at room temperature (RT) for 30 min. Cells were then harvested by centrifugation for 2 min at 8000 × g, resuspended in 1 ml FACS staining buffer containing 0.5 μM Sytox Green Nucleic acid stain (Life Technologies), and incubated at RT in the dark for 5 min. Samples were analyzed in flow cytometer (FACS Calibur, BD Biosciences) at laser excitation of 488 nm. Percentage of gated G1 cells of each strain was then normalized using gated G1 cells of the wild-type strain as reference.

Detection of intracellular (p)ppGpp levels

(p)ppGpp levels were visualized as described previously in (15) for *C. crescentus* (Cc) and in (16,17) for *S. meliloti*. Briefly, strains were grown overnight in PYE and then diluted for a second overnight culture in M5GG (Cc) or grown overnight in LBMC medium. Then, cells were diluted a second time in M5GG (Cc) or in LBMC medium and grown for 3 h to reach an OD_{660} of 0.5 (Cc) or 0.7. Cells were then split into two parts and washed twice with P5G-labelling buffer (Cc (15)) or with MOPS-MGS without glutamate (morpholine propane sulfonic acid; pH 7.4), 55 mM mannitol, 1 mM MgSO4, 0.25 mM CaCl2 and 0.004 mM biotin) (19). One milliliter of cells were then resuspended in 225 μl of P5G-labelling (-N) or M5G-labelling (+N) for *C. crescentus* and in 225 μl of MOPS-MGS with (+N) or without (-N) glutamate and 0.05% NH_4^+ for *S. meliloti*. In addition, media were supplemented with 25 μl of $KH_2{}^{32}PO_4$ at 100 μCi ml^{-1} and incubated for 1 h or 2 h (Cc) with shaking at 30°C. Then, samples were extracted with an equal volume of 2 M formic acid, placed on ice for 20 min and then stored overnight at −20°C. All cell extracts were pelleted at 14 000 rpm (18 000 x g) for 3 min and 6 × 2 μl (Cc) or 3 × 2 μl of supernatant were spotted onto a polyethyleneimine (PEI) plate (Macherey-Nagel). PEI plates were then developed in 1.5 M KH_2PO_4 (pH 3.4) at RT. Finally, thin layer chromatography (TLC) plates were imaged on a MS Storage Phosphor Screen (GE Healthcare) and analysed with Cyclone Phosphor Imager (PerkinElmer). For hydrolase experiments (Figure 3C), cells were incubated 1 h in P5G supplemented with xylose (0.1%). Then, cells were washed twice with P5G-labelling, resuspended in P5G-labelling supplemented with $KH_2{}^{32}PO_4$, xylose (0.1%) and glutamine (9.3 mM) and incubated for 2 h.

β-galactosidase assay

The β-galactosidase assays performed to measure P_{spoT}-*lacZ* activity were essentiality done as for the BTH assay with the following modifications. One milliter of *Caulobacter* strains harbouring the P_{spoT}-*lacZ* fusion was resuspended in 800 μl of Z buffer and the absorbance of the cultures at 660 nm (OD_{660}) instead of 590 nm was measured before the β-galactosidase assays. All the experiments were performed with three biological replicates and were normalized according to the wild-type strain harbouring the P_{spoT}-*lacZ* fusion cultivated at 30°C.

Immunoblot analysis

Immunoblot analyses were performed as described in (20) with the following primary antibodies: anti-MreB (1:5000) (20), anti-SpoT (1:5000) and secondary antibodies: anti-rabbit linked to peroxidase (GE Healthcare) at 1:5000, and visualized thanks to Western Lightning Plus-ECL chemiluminescence reagent (Biorad) and Amersham Imager 600 (GE Healthcare).

Proteins purification

Genes encoding *C. crescentus* SpoT, $SpoT_{D81G}$, $SpoT_{1–373}$, $SpoT_{\Delta ACT}$, SpoT ACT domain as well as $EI^{Ntr}{}_{\Delta GAF}$, HPr, $EIIA^{Ntr}$, $EIIA^{Ntr}{}_{H66E}$ and $EIIA^{Ntr}{}_{H66A}$ were transformed into *E. coli* BL21 (DE3) for protein production.

Each protein contains an N-terminal 6His-tag for purification by Ni-NTA chromatography. Cells were grown to an OD_{600} of ∼0.7 in LB medium (1 l) at 37°C. IPTG was added to a final concentration of 0.5 mM and incubated overnight at 28°C. Cells were harvested by centrifugation for 20 min at 4000 × g, 4°C, resuspended in 8 mM KCl, 1 mM tris(2-carboxyethyl)phosphine (TCEP), 2 mM $MgCl_2$, 50 mM Tris at pH 8, Protease Inhibitor Cocktail (Roche) and lysed with a cell disruptor at 60 psi in 500 mM KCl, 2 mM TCEP, 50 mM Tris at pH 8, 500 mM NaCl, 1% glycerol, Protease Inhibitor Cocktail. The lysis extract was centrifuged for 20 min at 40 000 × g, 4°C. Supernatants were loaded onto a HisTrap HP 1 ml column (GE Healthcare) in 50 mM 4-(2-hydroxyethyl)-1-piperazineethanesulfonic acid (HEPES), 500 mM KCl, 500 mM NaCl, 2 mM $MgCl_2$, 1 mM TCEP, 2% glycerol, 0.002% mellitic acid, Protease Inhibitor Cocktail (Roche), 5 mM imidazole, pH 7.5 and eluted with imidazole. The fractions recovered from the Ni-NTA were further purified by size exclusion chromatography (Superdex 200, for SpoT, $SpoT_{D81G}$, $SpoT_{1–373}$, $SpoT_{\Delta ACT}$ and $EI^{Ntr}{}_{\Delta GAF}$, and Superdex 75 for SpoT ACT domain, HPr, $EIIA^{Ntr}$, $EIIA^{Ntr}{}_{H66E}$ and $EIIA^{Ntr}{}_{H66A}$). Purified samples of SpoT were also used to immunize rabbits in order to produce anti-SpoT polyclonal antibodies.

In vitro phosphorylation of $EIIA^{Ntr}$

To produce phosphorylated $EIIA^{Ntr}$ ($EIIA^{Ntr}$∼P), $EI^{Ntr}{}_{\Delta GAF}$, HPr and $EIIA^{Ntr}$ were mixed at final concentrations of 2.5, 2.5 and 50 μM, respectively, in phosphorylation buffer [25 mM Tris pH 7.4, 10 mM KCl, 10 mM $MgCl_2$, 1 mM dithiothreitol (DTT)] and incubated at 37°C for 10 min. Samples concentrations were determined by absorbance measurement at 280 nm. The phosphorylation mix was then incubated in 2 mM of phosphoenopyruvate (PEP) at 37°C for 30 min. $EIIA^{Ntr}$∼P was further purified by size exclusion chromatography on a Superdex 75 and dialyzed for 72 h at 4°C, in 50 mM HEPES, 500 mM KCl, 500 mM NaCl, 2 mM $MgCl_2$, 1 mM TCEP, 2% glycerol and stored in 20% glycerol at −20°C.

In vitro hydrolase assay

To assess SpoT hydrolase activity, ^{32P}ppGpp was synthesized by enzymatic reaction catalyzed by RelA from *Chlorobaculum tepidum*. To synthesize ^{32P}ppGpp, 1 μM of $RelA_{Ctep}$ was incubated in 1 mM TCEP, 1 mM $MgCl_2$, 50 mM NaCl, 10 mM Tris at pH 7.4. Then, 100 μM guanosine diphosphate (GDP) were added to the synthesis reaction and incubated for 10 min at 37°C, followed by an addition of 3 pM [γ^{32}P] adenosine triphosphate (ATP) (PerkinElmer) incubated for 45 min, 37°C. ^{32P}ppGpp was extracted from the reaction medium by centrifugation in Amicon 3K Centrifugal filter (Millipore) at 13 000 × g for 25 min. The hydrolase assays were performed by incubating for 10 min at 37°C (i) 2 μM of $SpoT_{1–373}$ or $SpoT_{\Delta ACT}$ (Figure 4A), (ii) 1 μM of SpoT with increasing concentrations of $EIIA^{Ntr}$ or $EIIA^{Ntr}{}_{H66E}$ (5, 10 and 20 μM) (Figure

4B), (iii) 1 μM of SpoT with 20 μM of purified EIIA^{Ntr}∼P (Supplementary Figure S4a) or (iv) 1 μM of SpoT with or without EI$^{Ntr}{}_{\Delta GAF}$, HPr and EIIA^{Ntr} (5 μM each) (Figure 4C). Samples concentrations were determined by absorbance measurement at 280 nm. Then, 10 μl of ^{32P}ppGpp were added to the reaction mix to reach a final volume of 30 μl. The reaction was stopped by adding 2 μl of 12 M formic acid. Reaction products were separated by TLC by transferring 2 μl of the reaction medium onto a TLC PEI Cellulose F membrane (Millipore). Chromatography membranes were placed in 1 M of KH_2PO_4 buffer, pH 3.0, for 50 min at RT. The dried TLC membrane was placed in a Phosphor Screen plate (GE Healthcare) for 1 h and the Phosphor Screen revealed with a phosphoimager.

Isothermal Titration Calorimetry (ITC) assay

To measure the interaction between the ACT domain of SpoT and EIIA^{Ntr}∼P, EIIA$^{Ntr}{}_{H66E}$ or EIIA$^{Ntr}{}_{H66A}$, purified proteins were concentrated by centrifugation in Amicon 3K Centrifugal filter (Millipore) at 4000 × g, placed in Slide-A-Lyzer 3500 MWCO Dialysis Cassettes (ThermoScientific) and dialyzed in 50 mM HEPES, 500 mM KCl, 500 mM NaCl, 2 mM $MgCl_2$, 1 mM TCEP, 2% glycerol, 0.002% mellitic acid, Protease Inhibitor Cocktail (Roche), pH 7.5 during 24 h. Proteins were diluted to reach a final concentration of ∼110 μM (EIIA^{Ntr}∼P, EIIA$^{Ntr}{}_{H66E}$ and EIIA$^{Ntr}{}_{H66A}$) or 8 μM (SpoT ACT domain), degassed and equilibrated at titration temperature. Samples concentrations were determined by absorbance measurement at 280 nm. Isothermal Titration Calorimetry (ITC) measurements were performed with an Affinity ITC calorimeter (TA instruments) at 25°C, with a stirring rate of 75 rpm. A constant volume of 2 μl titrant was injected into the cell (177 μl) with an injection interval time of 250 s.

RESULTS

EIIA^{Ntr}∼P interacts directly with the ACT domain of SpoT

We showed previously that only the phosphorylated version of *C. crescentus* EIIA^{Ntr} (EIIA^{Ntr}∼P) was able to interact with SpoT in a BTH assay (15). To map the domains of SpoT interacting with EIIA^{Ntr}∼P, we used truncated versions of SpoT in a BTH assay (Figure 1A). We found that deleting the ACT domain (SpoT$_{\Delta 668–719}$, referred to as SpoT$_{\Delta ACT}$ throughout the manuscript) precluded the interaction with EIIA^{Ntr}∼P as well as with the isolated ACT domain (ACT$_{506–742}$), but not with full-length SpoT (Figure 1B and Supplementary Figure S1a). Moreover, the ACT domain alone was able to strongly interact with EIIA^{Ntr}∼P (Figure 1B and Supplementary Figure S1a) as well as with itself (Supplementary Figure S1b). Together, these results suggest that the ACT domain is sufficient to mediate the interaction between SpoT and EIIA^{Ntr}∼P.

Inactivating the ACT domain increases (p)ppGpp levels

Disrupting the interaction between SpoT and EIIA^{Ntr}∼P should release the hydrolase activity of SpoT, since strains

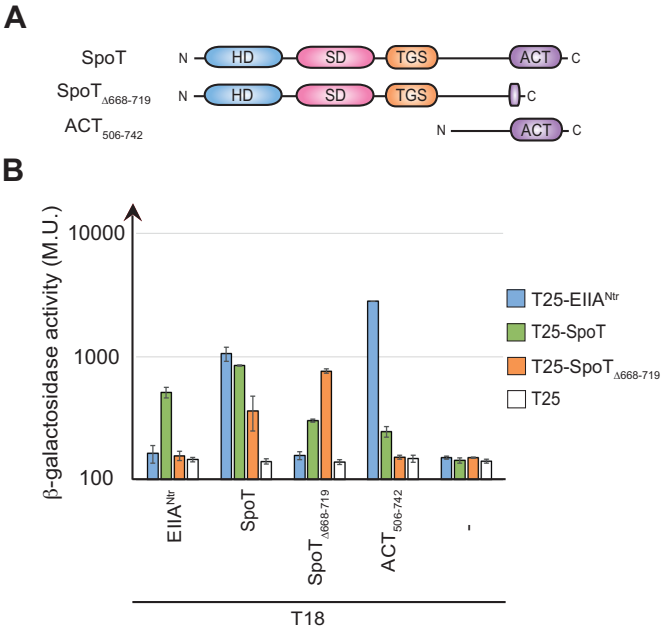

Figure 1. The ACT domain is required for the interaction between SpoT and EIIA^{Ntr}∼P in a bacterial two-hybrid assay. (**A**) Domain organisation of *C. crescentus* SpoT with the catalytic domains, HD and SD, located at the N-terminal extremity and the regulatory domains, TGS and ACT, located at the C-terminal end. The SpoT variants used in the BTH assay (SpoT$_{\Delta 668–719}$ and ACT$_{506–742}$) are also represented. (**B**) SpoT and ACT$_{506–742}$, but not SpoT$_{\Delta 668–719}$, directly interact with EIIA^{Ntr}∼P. β-galactosidase assays were performed on MG1655 *cyaA::frt* (RH785) strains coexpressing T18- fused to *ptsN, spoT*, *spoT*$_{\Delta 668–719}$ or *ACT*$_{506–742}$ with T25- fused to *ptsN*, *spoT* or *spoT*$_{\Delta 668–719}$. Error bars = SD, $n = 3$.

that either did not express EIIA^{Ntr} (Δ*ptsN*) or expressed only the non-phosphorylated form of EIIA^{Ntr} (Δ*ptsP*, Δ*ptsH* or *ptsN*$_{H66A}$) increased (p)ppGpp hydrolysis *in vivo* (15). Accordingly, a *C. crescentus* strain expressing *spoT*$_{\Delta ACT}$ as the only copy of *spoT* might phenocopy the Δ*ptsP* strain by decreasing motility and shortening G1 lifetime (15). Surprisingly, we found that *spoT*$_{\Delta ACT}$ cells phenocopied rather the hydrolase-dead mutant *spoT*$_{D81G}$ than Δ*ptsP* (15). Indeed, the *spoT*$_{\Delta ACT}$ mutation led to an increase of motility, an accumulation of G1/swarmer cells and a growth delay in PYE complex medium (Figure 2A–D). As for *spoT*$_{D81G}$, these phenotypes might be due to a (p)ppGpp excess in *spoT*$_{\Delta ACT}$. In support of this, *spoT*$_{\Delta ACT}$ cells accumulated (p)ppGpp without stress (Figure 2E). In addition, abolishing the synthetase activity in *spoT*$_{\Delta ACT}$ cells, either by deleting *ptsP* (EI^{Ntr}) or by incorporating a Y323A substitution into SpoT (*spoT*$_{Y323A\ \Delta ACT}$) known to specifically inactivate synthetase activity (15,21), suppressed all the phenotypes (Figure 2A–E and Supplementary Figure S2a).

We observed that SpoT$_{\Delta ACT}$ and SpoT$_{D81G}$ protein levels in the corresponding mutant strains were slightly higher than the SpoT level in the wild-type strain (Supplementary Figure S2b,c). Nevertheless, upon nitrogen starvation, (p)ppGpp levels in *spoT*$_{\Delta ACT}$ were slightly lower than in wild-type cells (Supplementary Figure S2d). The slight increase of SpoT$_{\Delta ACT}$ and SpoT$_{D81G}$ levels is likely a result of the positive feedback loop of (p)ppGpp on *spoT* promoter.

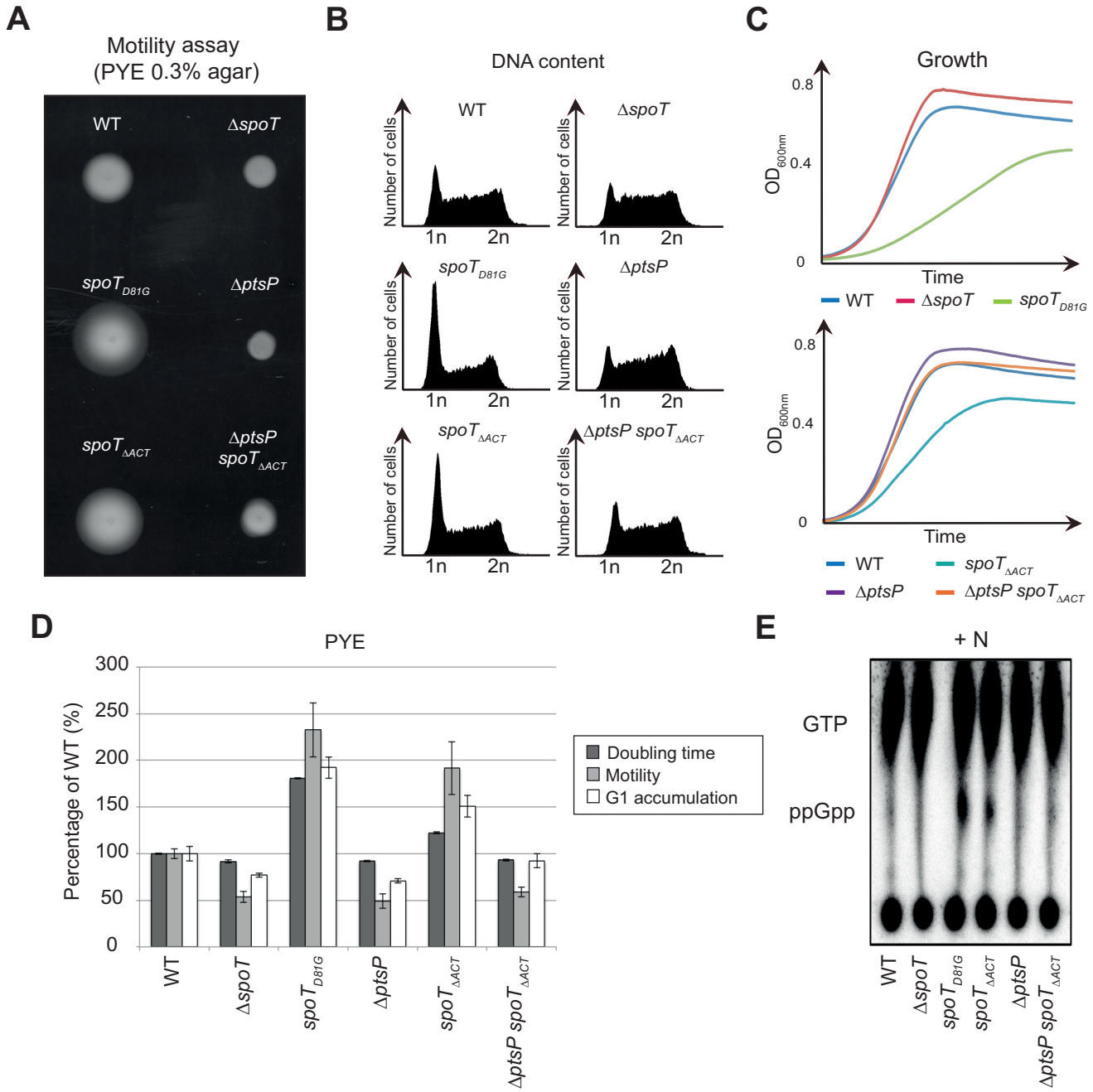

Figure 2. Inactivation of the ACT domain of SpoT leads to (p)ppGpp accumulation, which consequently extends the G1/swarmer cell lifetime of *C. crescentus*. (**A**–**D**) Extension of the G1/swarmer lifetime in $spoT_{\Delta ACT}$ cells is suppressed by inactivating *ptsP* (encoding EI^{Ntr}). Motility (A), DNA content (B) and growth (C) were measured in WT (RH50), Δ*spoT* (RH1755), $spoT_{D81G}$ (RH1752), Δ*ptsP* (RH1758), $spoT_{\Delta ACT}$ (RH1476) and Δ*ptsP* $spoT_{\Delta ACT}$ (RH1478) strains grown in complex media PYE. (D) Data shown in a-c were normalized to the WT (100%). Error bars = SD, $n = 3$. (**E**) Inactivation of the ACT domain leads to (p)ppGpp accumulation. The intracellular levels of (p)ppGpp were evaluated by TLC after nucleotides extraction from the same strains grown in nitrogen-replete (+N) conditions.

Indeed, P_{spoT} displayed higher activity in strains accumulating (p)ppGpp (*ptsP*$_{L83Q}$ and P_{xylX}::*relA-FLAG*) and lower activity in ppGpp^0 strains (Δ*ptsP,* Δ*ptsH and* Δ*ptsN*), so that SpoT protein levels varied according to (p)ppGpp levels (Supplementary Figure S2e-g). Together, our data suggest that ACT might be required for SpoT hydrolase activity.

The hydrolase activity of SpoT requires the ACT domain

To test whether ACT was required for (p)ppGpp hydrolysis, we first measured (p)ppGpp hydrolysis *in vivo* (15). To this end, we used *C. crescentus* strains in which (p)ppGpp (i) cannot be produced anymore by the endogenous SpoT since its synthetase activity has been inactivated with the Y323A mutation (15,21), but (ii) can be synthe-

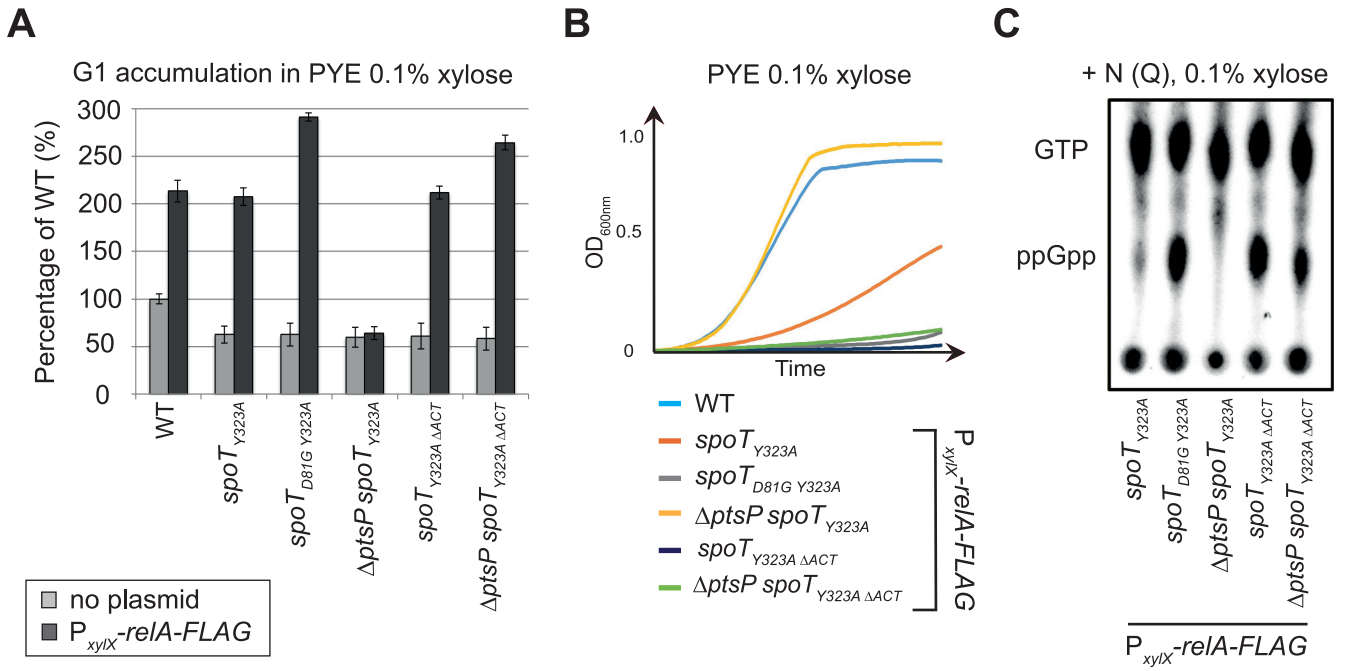

Figure 3. The ACT domain is required *in vivo* to support the hydrolase activity of SpoT. (**A** and **B**) Absence of the ACT domain of SpoT promotes G1 accumulation and decreases growth rate upon artificial exogenous production of (p)ppGpp. (A) Flow cytometry analysis to determine DNA content in asynchronous population of WT (RH50), *spoT*$_{Y323A}$ (RH1844), *spoT*$_{D81G\ Y323A}$ (RH2193), Δ*ptsP spoT*$_{Y323A}$ (RH2196), *spoT* $_{Y323A\ \Delta ACT}$ (RH1586) and Δ*ptsP spoT* $_{Y323A\ \Delta ACT}$ (RH2492) strains with (black bars) or without (grey bars) P$_{xylX}$*::relA-FLAG* grown for 6 h in PYE medium supplemented with 0.1% of xylose. The flow cytometry data were normalized to the WT without P$_{xylX}$*::relA-FLAG* (100%). (B) The growth of strains used in (A) was measured for 24 h in PYE medium supplemented with 0.1% of xylose. Error bars = SD, $n = 3$. (**C**) The regulatory ACT domain of SpoT is required *in vivo* to degrade (p)ppGpp in nitrogen-replete condition (+N). The intracellular levels of (p)ppGpp were evaluated by TLC after nucleotides extraction from *spoT*$_{Y323A}$ (RH1844), *spoT*$_{D81G\ Y323A}$ (RH2193), Δ*ptsP spoT*$_{Y323A}$ (RH2196), *spoT*$_{Y323A\ \Delta ACT}$ (RH1586) and Δ*ptsP spoT*$_{Y323A\ \Delta ACT}$ (RH2492) strains harbouring P$_{xylX}$*::relA-FLAG* and grown for 2 h in glutamine (Q) containing media (+N) supplemented with 0.1% xylose.

sized upon addition of xylose by a truncated version of the *E. coli* RelA (p)ppGpp synthetase expressed from the xylose-inducible promoter (P$_{xylX}$*::relA-FLAG*) at the *xylX* locus (14). Thus, in these strains the only hydrolase activity capable to degrade (p)ppGpp produced by *E. coli* RelA was supplied by endogenous SpoT variants. Note that, as expected, all the strains harbouring the *spoT*$_{Y323A}$ mutation but without P$_{xylX}$*::relA-FLAG* had a G1 proportion lower than the WT, because they did not produce (p)ppGpp (Figure 3A). In agreement with our previous observations, inactivation of SpoT hydrolase in such a background (*spoT*$_{D81G\ Y323A;}$P$_{xylX}$*::relA-FLAG*) led to a strong (p)ppGpp accumulation, an extension of the G1 phase and a growth arrest (Figure 3 and (15)). In contrast, releasing SpoT hydrolase activity (Δ*ptsP spoT*$_{Y323A;}$P$_{xylX}$*::relA-FLAG*) led to undetectable levels of (p)ppGpp, a reduced G1 phase and an optimal growth (Figure 3 and (15)). Interestingly, deleting the ACT domain of SpoT (*spoT*$_{Y323A\ \Delta ACT;}$P$_{xylX}$*::relA-FLAG*) led to a (p)ppGpp accumulation, a G1 proportion and a growth rate similar to the hydrolase-dead mutant (*spoT*$_{D81G\ Y323A;}$P$_{xylX}$*::relA-FLAG*) and this independently of the presence of *ptsP* (Figure 3 and Supplementary Figure S3).

These data strongly suggest that the ACT domain is strictly required *in vivo* for (p)ppGpp hydrolysis and that EIIA^{Ntr}∼P inhibits this activity by interfering with the ACT domain of SpoT. To test these hypotheses, we performed *in vitro* ppGpp hydrolysis assays with the full-length enzyme and mutants lacking either the entire C-terminal regulatory domains (SpoT$_{1–373}$) or only the ACT domain (SpoT$_{\Delta 668–719}$). We observed that full-length SpoT could efficiently hydrolyze [^{32}P]ppGpp but the deletion of the ACT domain in both ACT-deficient SpoT variants strongly affected the hydrolase activity. Indeed, radiolabelled [^{32}P]ppGpp remained mostly intact in the presence of SpoT$_{\Delta ACT}$ (84% ± 4%) or SpoT$_{1–373}$ (89% ± 11%), whereas more than 90% of [^{32}P]ppGpp were hydrolyzed by the full-length SpoT (Figure 4A). To check whether phosphorylated EIIA^{Ntr} could modulate the hydrolase activity of SpoT, [^{32}P]ppGpp hydrolysis was first measured in the presence of the WT (EIIA^{Ntr}), a phospho-dead (EIIA$^{Ntr}_{H66A}$) or a phosphomimetic (EIIA$^{Ntr}_{H66E}$) version of EIIA^{Ntr}. We found that EIIA$^{Ntr}_{H66E}$ interfered with the SpoT hydrolase activity, in contrast to EIIA$^{Ntr}_{H66A}$ and EIIA^{Ntr} that had only a slight effect on the activity of the enzyme (Figure 4B). It is noteworthy that WT EIIA^{Ntr} has a residual inhibition activity of SpoT at high concentration (20 μM). This dose-dependent effect was not observed with EIIA$^{Ntr}_{H66E}$ (Figure 4B), suggesting that a certain amount of the EIIA^{Ntr} population is phosphorylated in *E. coli* and remains stable after purification. Indeed, it has been shown that *E. coli* EIIA^{Ntr} remains phosphorylated after purification (22,23) and *Caulobacter* EIIA^{Ntr} can be phosphorylated *in vivo* in *E. coli* (15). Together these data suggest that phosphorylation of EIIA^{Ntr} is required to inhibit (p)ppGpp hydrolysis by SpoT. To challenge this hypothesis, we performed *in vitro*

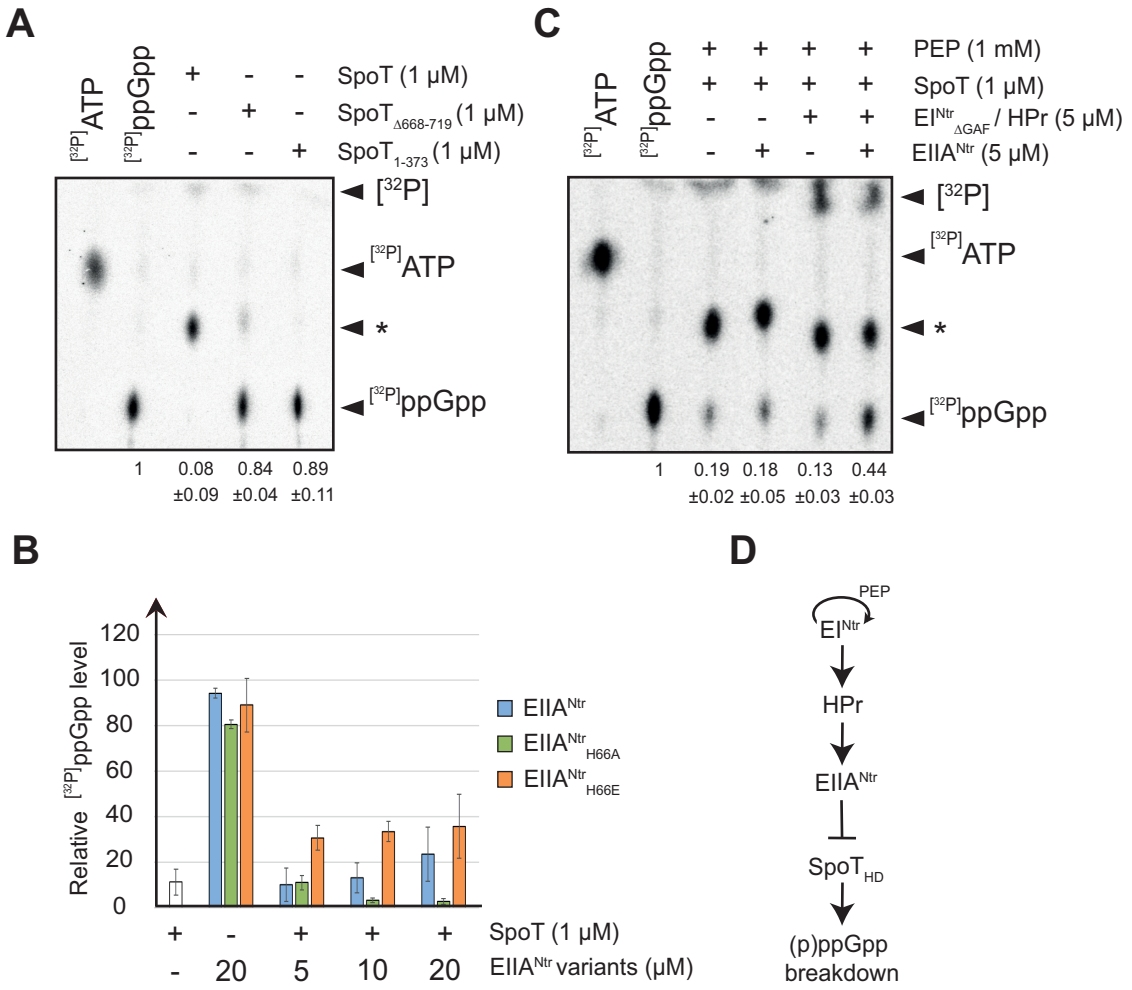

Figure 4. EIIA^{Ntr}∼P inhibits the hydrolase activity of SpoT *in vitro* in an ACT-dependent way. (**A**) The ACT domain of SpoT is required to hydrolyze ppGpp. Radiolabelled [32P]ppGpp incubated with 1 μM of SpoT, SpoT$_{Δ668–719}$ or SpoT$_{1–373}$ was separated by TLC. (**B**) Phosphomimetic variant of EIIA^{Ntr} (EIIA$^{Ntr}_{H66E}$) inhibits the hydrolase activity of SpoT. Radiolabelled [32P]ppGpp incubated with 1 μM of SpoT in the presence of increasing concentrations (5, 10 and 20 μM) of unphosphorylated EIIA^{Ntr}, phospho-dead EIIA$^{Ntr}_{H66A}$ or phosphomimetic EIIA$^{Ntr}_{H66E}$ variants was separated by TLC. [32P]ppGpp incubated with EIIA^{Ntr} variants alone were added as controls. The data were normalized to the signal for [32P]ppGpp incubated alone without proteins (100%). (**C**) Phosphorylated EIIA^{Ntr} protects ppGpp from hydrolysis by SpoT. Radiolabelled [32P]ppGpp incubated with 1 μM of SpoT in the presence of EIIA^{Ntr} (5 μM) with or without EI$^{Ntr}_{ΔGAF}$ (5 μM) and HPr (5 μM) was separated by TLC. The star '*' indicates a [32P]ppGpp intermediate degradation. [32P]ATP and [32P]ppGpp were used as references. Relative amounts of [32P]ppGpp are indicated below each lane of TLC. Error bars = SD, $n \geq 3$ for (A-C). (**D**) Schematic representation of the PTS^{Ntr} pathway in *C. crescentus* showing that phosphorylated EIIA^{Ntr} inhibits SpoT hydrolase activity.

hydrolase assays with a reconstituted PTS^{Ntr} system (PEP, EI^{Ntr}, HPr and EIIA^{Ntr}). Note that EIIA^{Ntr} can be phosphorylated on His66 in this condition only in the presence of PEP, EI^{Ntr} and HPr (data not shown). We found that more than 40% of [32P]ppGpp was protected from hydrolysis by SpoT when incubated with all the PTS^{Ntr} members whereas the same mix but lacking EIIA^{Ntr} did not inhibit SpoT hydrolase activity (Figure 4C). Likewise, incubating SpoT with repurified EIIA^{Ntr}∼P once phosphorylated *in vitro* interfered with [32P]ppGpp degradation in comparison to unphosphorylated EIIA^{Ntr} (Supplementary Figure S4a). Moreover, phosphorylation of EIIA^{Ntr} increased its affinity for the ACT domain of SpoT (Supplementary Figure S4b). This not only supports that phosphorylation enhances *in vivo* binding of EIIA^{Ntr} to the ACT domain (Figure 1B and Supplementary Figure S1a), but also explains why SpoT hydrolase activity was not inhibited by non-phosphorylated EIIA^{Ntr}. Altogether, these data suggest that EIIA^{Ntr}∼P interacts with the ACT domain to inhibit hydrolase activity of SpoT (Figure 4D).

PTS^{Ntr} regulates (p)ppGpp accumulation in *Sinorhizobium meliloti*

The inhibition of EI^{Ntr} autophosphorylation by glutamine was first observed in the γ-proteobacterium *E. coli* (24) and the plant-associated α-proteobacterium *S. meliloti* (25). In addition, *S. meliloti* also accumulates (p)ppGpp in response to nitrogen starvation (16,17). This suggests that PTS^{Ntr} might also stimulate (p)ppGpp accumulation in *S. meliloti* in response to glutamine deprivation as shown for *C. crescentus* (15). To test this hypothesis, we checked whether the nitrogen-related EIIA component of *S. meliloti* (EIIA^{Ntr})

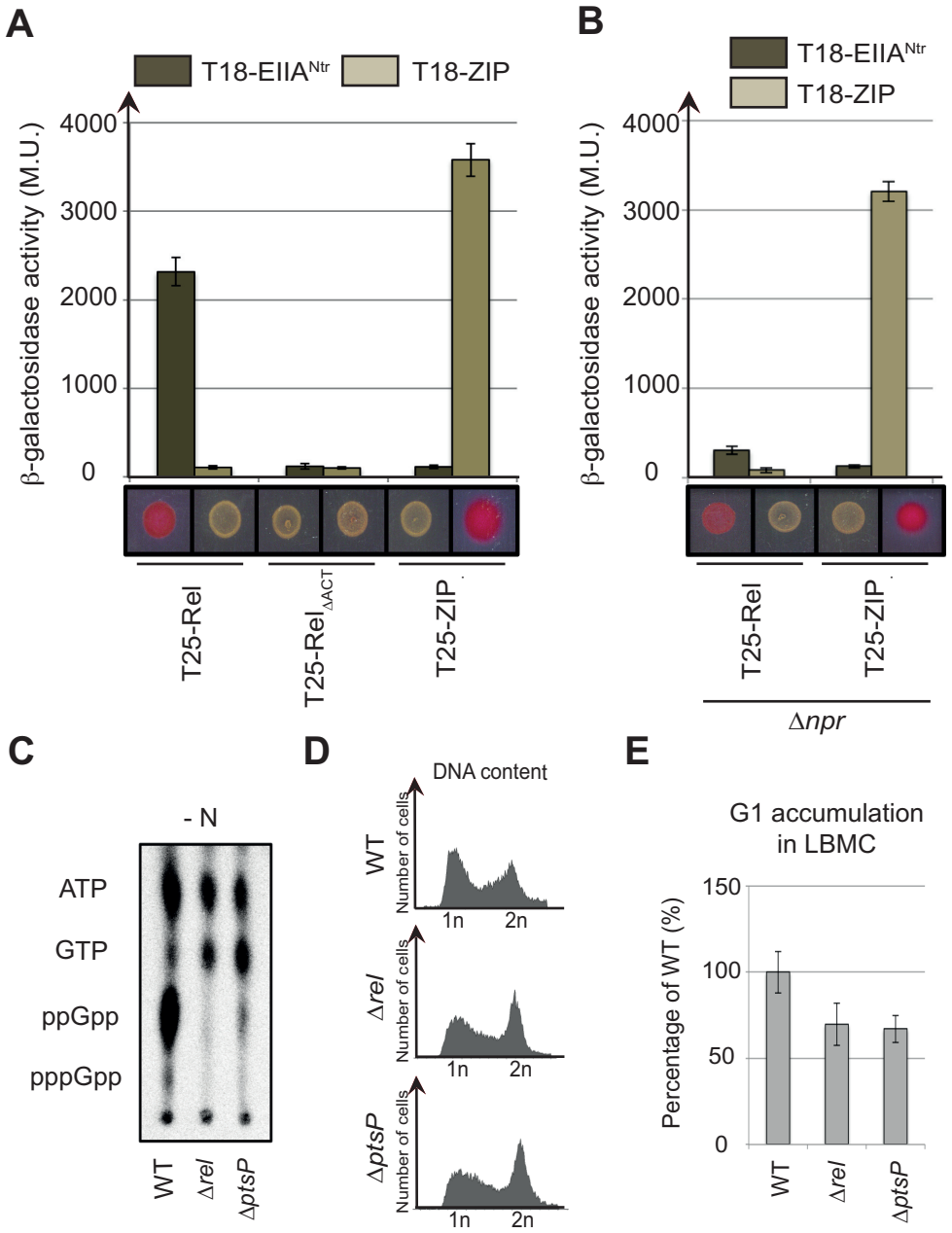

Figure 5. PTS^{Ntr} modulates (p)ppGpp accumulation and cell cycle progression in *S. meliloti*. (**A** and **B**) EIIA^{Ntr} interacts with Rel in an ACT-dependent way. β-galactosidase assays were performed on (A) MG1655 *cyaA::frt* (RH785) or (B) MG1655 *cyaA::frt* Δ*npr* (RH2122) strains coexpressing T18- fused to *ptsN* or *ZIP* with T25- fused to *rel*, *rel*$_{\Delta ACT}$ or *ZIP*. Error bars = SD, $n = 3$. The same strains were spotted on MacConkey Agar Base plates supplemented with 1% maltose. Plates were incubated for 1 day at 30°C. The red colour indicates positive interactions. (**C**–**E**) A functional PTS^{Ntr} is required for (p)ppGpp accumulation in *S. meliloti* upon nitrogen starvation (-N) and for cell cycle progression in nitrogen-replete (+N) condition. (C) The intracellular levels of (p)ppGpp were evaluated by TLC after nucleotides extraction from WT (RH2000), Δ*rel* (RH2327) and Δ*ptsP* (RH2326) strains grown for 6 h without nitrogen source (-N). (D-E) DNA content (D) and G1 proportion (E) were measured in the same strains grown in complex media (LBMC). G1 proportions were normalized to the WT (100%). Error bars = SD, $n = 3$.

was able to interact with the bifunctional (SD/HD) RSH of *S. meliloti* (Rel) in a BTH assay. As shown in Figure 5A, the full-length Rel fused to T25 (T25-Rel) interacted with EIIA^{Ntr} fused to T18 (T18-EIIA^{Ntr}). Similarly to *C. crescentus*, the deletion of ACT (T25-Rel$_{\Delta ACT}$) abolished this interaction (Figure 5A). Another conserved feature is that phosphorylation of EIIA^{Ntr} enhanced interaction with Rel. Indeed, we previously showed that (i) EIIA^{Ntr} was phosphorylated in the BTH assay by the endogenous PTS^{Ntr} system of *E. coli* (EI^{Ntr} and NPr) and (ii) the interaction between SpoT and EIIA^{Ntr} was altered in an *E. coli* Δ*npr* background (15). Likewise, the interaction between *S. meliloti* T18-EIIA^{Ntr} and T25-Rel was strongly diminished in a Δ*npr* background (Figure 5B), indicating that phosphorylation of EIIA^{Ntr} also enhances the interaction with Rel.

We constructed single in-frame deletion of *ptsP* (SMc02437) and *rel* (SMc02659) genes to test the PTS^{Ntr}-dependent accumulation of (p)ppGpp in *S. meliloti* in response to nitrogen deprivation. Upon nitrogen starvation (-N), neither *Δrel* nor *ΔptsP* cells accumulated (p)ppGpp in contrast to wild-type cells (Figure 5C). The increase of G1 proportion that results from the accumulation of (p)ppGpp upon nutrient limitation was previously used to synchronize *S. meliloti* (26). Thus, if PTS^{Ntr} regulates (p)ppGpp levels, we reasoned that the G1 proportion of *Δrel* and *ΔptsP* populations should be reduced. This is exactly what we observed, with a proportion of G1 cells in the *ΔptsP* and *Δrel* strains reduced in comparison to the wild-type strain (Figure 5D and E). In contrast, the ectopic production of (p)ppGpp in unstarved *S. meliloti* cells with an IPTG-inducible version of $RelA_{Ec}$ strongly increased the proportion of G1 cells and led to growth arrest (Supplementary Figure S5). Altogether, these results support a conserved role of PTS^{Ntr} in regulating (p)ppGpp accumulation in response to nitrogen starvation as well as in the control of cell cycle progression in *S. meliloti*.

DISCUSSION

Two decades ago, mutational analysis of the *spoT* gene of *E. coli* suggested that the C-terminal end of SpoT including the ACT domain was an anchor point for regulators of the hydrolase activity of SpoT (27). Later, Mechold *et al.* reported that deleting the CTD of SpoT in *Streptococcus equisimilis* led to a strong inhibition of (p)ppGpp hydrolysis *in vitro* of ∼150-fold in comparison to the full-length enzyme (28). In agreement with these studies, our work shows that the ACT domain modulates SpoT hydrolase activity in *C. crescentus*. In a nitrogen-rich environment (+N), the ACT domain stimulates hydrolase activity, thereby limiting (p)ppGpp concentration. Upon nitrogen starvation (-N), the last component of the nitrogen-related PTS (PTS^{Ntr}), $EIIA^{Ntr}$, is phosphorylated and binds to the ACT domain of SpoT. This interaction likely interferes with the ACT-dependent stimulation of SpoT hydrolase activity, thereby inhibiting (p)ppGpp hydrolysis (Figure 6). The recent RelA structures on stalled ribosomes highlighted the role of CTD in sensing nutrient availability (5–7). When bound to the ribosome, RelA adopts an extended conformation, which is thought to relieve the inhibitory effect of the CTD on its synthetase activity and enhances (p)ppGpp synthesis (29). This extended conformation seems to be favoured by specific interactions between the ribosome stalk, the A-site finger and the tRNAs with the CTD (7). Given the conserved domain architecture of the long RSH proteins, we propose that $EIIA^{Ntr}$∼P modulates SpoT/Rel conformation to decrease its hydrolase activity (Figure 6). As ACT seems to interact with itself, it is tempting to speculate that dimerization of ACT induces a conformation that enhances the hydrolase activity. Oligomerization of long RSH has already been proposed to regulate their activity (29,30). For instance, mutations in the bifunctional Rel of *Mycobacterium tuberculosis* that lead to monomerization of Rel were shown to increase synthetase activity (30). Nevertheless, the $SpoT_{\Delta ACT}$ variant can still homo-dimerize in a BTH assay (Figure 1 and Supplementary Figure S1), thereby ruling out the hypothesis that inactivation of hydrolase activity is simply due to monomerization of SpoT/Rel. Indeed, our data show that SpoT harbours at least two multimerization domains, (i) ACT at the C-terminal end and (ii) another one located in the N-terminal catalytic domains (Figure 1 and our unpublished data). Note that the N-terminal extremity of *M. tuberculosis* Rel harbouring the catalytic domains was already shown to homo-dimerize (31). In addition, the ACT alone can interact with full length SpoT but not with $SpoT_{\Delta ACT}$ (Figure 1 and Supplementary Figure S1), showing that the ACT domain unlikely interferes directly with HD. Thus, the multimerization of C-terminal ACT might rather induce a conformational change of the catalytic domains located at the N-terminal extremity, favouring the hydrolase over the synthetase activity. In such a scenario, $EIIA^{Ntr}$∼P might compete with ACT multimerization to preclude or interfere with an active conformational state favourable for (p)ppGpp hydrolysis. Whatever the mechanism(s) used, the role of the ACT domain in sustaining the hydrolase activity of long RSH enzymes might be conserved, since more than 88% of them harbour a C-terminal ACT domain (InterPro IPR002912).

The ACT domains have been shown to bind small molecules—mostly amino acids—and to regulate activity of the associated enzymatic domain (32). Recently, branched-chain amino acids (BCAAs)—valine and isoleucine—were found to bind the ACT domain of *Rhodobacter capsulatus* Rel (Rel_{Rc}) and to stimulate (p)ppGpp hydrolysis (33). However, even though *R. capsulatus* is also an α-proteobacterium, BCAAs do not bind *Caulobacter* SpoT protein (33). Interestingly, we found that the interaction between Rel and the phosphorylated form of $EIIA^{Ntr}$ also occurs in an α-proteobacterium very close to *R. capsulatus*, *Rhodobacter sphaeroides* (Supplementary Figure S6). This suggests that the *Rhodobacter* genus could use BCAAs and PTS^{Ntr} to regulate (p)ppGpp hydrolysis in response to different metabolic cues. The ACT of *E. coli* RelA was also shown to be in close contact with the A-site finger of 23S ribosomal RNA (rRNA) (5,6). Although we cannot exclude the possibility that ACT of *C. crescentus* SpoT also binds other small molecules than BCAAs and/or rRNA, we show here that the ACT domain interacts with the regulatory protein ($EIIA^{Ntr}$) to modulate its hydrolase activity. As the phosphorylation of $EIIA^{Ntr}$ that favoured interaction with ACT is inversely correlated with the glutamine concentration, this provides an elegant mechanism to tightly coordinate nutrient availability with the intracellular concentration of (p)ppGpp (15).

We also reported that $SpoT_{\Delta ACT}$ is still able to increase (p)ppGpp concentration upon nitrogen starvation—although to a lesser extent in comparison to SpoT—by stimulating its synthetase activity in a PTS^{Ntr}-dependent way (Supplementary Figure S2d). Although the ACT domain might also be required for an optimal synthetase activity, the TGS domain seems be more important for synthetase activity. Indeed, the deletion of the CTD harbouring the TGS and the ACT domains completely abolished the ability of *C. crescentus* SpoT to produce (p)ppGpp upon nitrogen starvation (10). As we showed that PTS^{Ntr} is required for synthesizing (p)ppGpp in *Caulobacter* cells starved for nitrogen (15) (Figure 6), it will

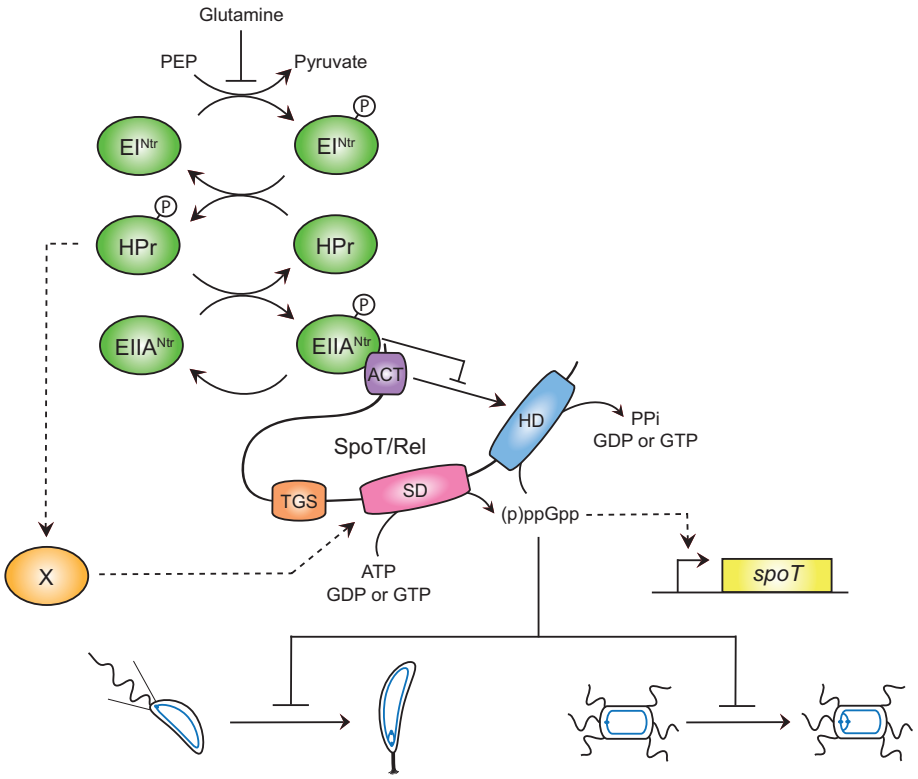

Figure 6. EIIA^{Ntr}∼P binds the ACT domain of SpoT and inhibits its hydrolase activity. Upon nitrogen starvation (i.e. glutamine deprivation), EI^{Ntr} phosphorylates its downstream components, HPr and EIIA^{Ntr}. As a consequence, EIIA^{Ntr}∼P interacts with ACT to likely inhibit its stimulating effect on the hydrolase activity of SpoT. This inhibition avoids to degrade (p)ppGpp produced by the SD, this latter being strongly stimulated by HPr∼P by an unknown mechanism. In addition, increasing the (p)ppGpp level promotes the accumulation of the SpoT protein by a positive feedback loop mechanism on transcription of the *spoT* gene. Ultimately, the burst of (p)ppGpp delays the G1-to-S transition of *C. crescentus* (left) and *S. meliloti* (right) cells.

be interesting to test *in vitro* if the PTS^{Ntr} also modulates the synthetase activity of SpoT/Rel and if TGS and/or ACT domains are required for this regulation.

The hydrolase activity of *E. coli* SpoT was recently shown to be activated by the anti-σ70 factor (Rsd) via a direct interaction with the TGS domain (34). Intriguingly, this Rsd-dependent control of (p)ppGpp hydrolysis is also regulated by the PTS. Indeed, unphosphorylated HPr was previously shown to interact with Rsd in order to sequester it and prevent activation of SpoT hydrolase activity (34,35). Since HPr phosphorylation is determined by carbon source availability in *E. coli*, the authors suggested that Rsd could balance (p)ppGpp levels during a carbon source downshift (34). All these examples together with our work illustrate the importance of the CTD in the regulation of catalytic activities (hydrolase and synthetase) of SpoT/Rel enzymes.

Besides *C. crescentus*, another α-proteobacterium, *S. meliloti*, uses PTS^{Ntr} to sense nitrogen starvation and to stimulate (p)ppGpp accumulation (Figure 6). We found that EIIA^{Ntr} interacts with Rel (Figure 5A) and that phosphorylation of EIIA^{Ntr} promotes this interaction (Figure 5B). As glutamine also inhibits phosphorylation of EI^{Ntr} in *S. meliloti* (25), glutamine deprivation likely leads to hyperphosphorylation of downstream PTS^{Ntr} components, favouring subsequent interaction between EIIA^{Ntr}∼P and Rel. In support of that, we showed *S. meliloti* required EI^{Ntr} protein to accumulate (p)ppGpp upon nitrogen starvation (Figure 5C), as previously shown for *C. crescentus* (15). Altogether, our data support that the PTS^{Ntr}-dependent control of Rel activities is another conserved feature in α-proteobacteria (36). But beyond α-proteobacteria, other bacterial phyla also use PTS proteins to determine (p)ppGpp levels accordingly to the metabolic status. As already mentioned, HPr can indirectly modulate the hydrolase activity of SpoT in the α-proteobacterium *E. coli* (34) whereas the unphosphorylated EIIA^{Ntr} protein directly interacts with a RSH enzyme in the β-proteobacterium *Ralstonia eutropha* (37).

Similarly to *C. crescentus* (14,15), we found that (p)ppGpp accumulation also delays the G1-to-S transition in *S. meliloti*, (Figure 5D and E; Supplementary Figure S5). In fact, this feature has been used to synchronize a population of *S. meliloti* by transiently blocking bacteria starved for carbon and nitrogen in G1 phase of the cell cycle (26). The alarmone was previously shown to be critical for *S. meliloti* to establish a symbiotic relationship with its host plant (17). Indeed, (p)ppGpp strongly influences transcription of hundreds of genes, thereby affecting multiple aspects of symbiosis such as nodulation or succinoglycan production (16). Interestingly, secondary mutations in RNA polymerase suppressed all the defects of a (p)ppGpp^0 strain, demonstrating that transcriptional control by the alarmone is critical for symbiosis (17). However, the (p)ppGpp-dependent control of the cell cycle might also

be critical for symbiosis. Indeed, it has been shown that the intracellular pathogen *Brucella abortus* uses specific cell cycle stage to promote invasion of macrophages, with G1 cells being the predominant infectious bacteria (38). Therefore, asymmetric cell division might have been conserved in α-proteobacteria (36) for the ability of the invasive newly divided G1 cells to efficiently colonize new environments, and (p)ppGpp might systematically control this adaptive feature. The specific interference of (p)ppGpp with the G1-to-S transition of the cell cycle could thus be another conserved feature in α-proteobacteria.

SUPPLEMENTARY DATA

Supplementary Data are available at NAR Online.

ACKNOWLEDGEMENTS

We are grateful to Sean Crosson, Emanuele Biondi and Gabriele Klug for providing strains and/or plasmids. We thank the members of the BCcD team for critical reading of the manuscript and helpful discussions; Guy Houbeau at the Animal Care Facility of the University of Namur for immunizing rabbits with purified SpoT.
Author contributions: S.R. and R.H. conceived and designed the experiments. S.R. performed all the experiments except otherwise stated. J.C-M. purified the proteins for the biochemical assays and performed the *in vitro* hydrolase assays, the phosphorylation of $EIIA^{Ntr}$ and ITC assays (Figure 4 and Supplementary Figure S4). J.C. did the experiments for the reviewing and A.M. did the cloning and preliminary tests for proteins purification and *in vitro* phosphorylation assays. S.R., J.C-M., A.G-P. and R.H. analysed the data. S.R. and R.H. wrote the paper.

FUNDING

Fonds de la Recherche Scientifique - FNRS (F.R.S.-FNRS) [CDR J.0169.16 to R.H.]; [EQP U.N043.17F; WELBIO CR-2017S-03; PDR T.0066.18 to A.G-P.]; Programme 'Actions de Recherche Concertée' 2016–2021 from the ULB and the Fonds d'Encouragement à la Recherche ULB (FER-ULB to A.G-P.); FRIA (Fund for Research Training in Industry and Agriculture) fellowships from the F.R.S.-FNRS to S.R. and J.C-M. R.H. is a Research Associate of the F.R.S.-FNRS. Funding for open access charge: University of Namur.
Conflict of interest statement. None declared.

REFERENCES

1. Hallez,R., Delaby,M., Sanselicio,S. and Viollier,P.H. (2017) Hit the right spots: cell cycle control by phosphorylated guanosines in alphaproteobacteria. *Nat. Rev. Microbiol.*, **15**, 137–148.
2. Hauryliuk,V., Atkinson,G.C., Murakami,K.S., Tenson,T. and Gerdes,K. (2015) Recent functional insights into the role of (p)ppGpp in bacterial physiology. *Nat. Rev. Microbiol.*, **13**, 298–309.
3. Potrykus,K. and Cashel,M. (2008) (p)ppGpp: still magical? *Annu. Rev. Microbiol.*, **62**, 35–51.
4. Haseltine,W.A. and Block,R. (1973) Synthesis of guanosine tetra- and pentaphosphate requires the presence of a codon-specific, uncharged transfer ribonucleic acid in the acceptor site of ribosomes. *Proc. Natl. Acad. Sci. U.S.A.*, **70**, 1564–1568.
5. Arenz,S., Abdelshahid,M., Sohmen,D., Payoe,R., Starosta,A.L., Berninghausen,O., Hauryliuk,V., Beckmann,R. and Wilson,D.N. (2016) The stringent factor RelA adopts an open conformation on the ribosome to stimulate ppGpp synthesis. *Nucleic Acids Res.*, **44**, 6471–6481.
6. Brown,A., Fernandez,I.S., Gordiyenko,Y. and Ramakrishnan,V. (2016) Ribosome-dependent activation of stringent control. *Nature*, **534**, 277–280.
7. Loveland,A.B., Bah,E., Madireddy,R., Zhang,Y., Brilot,A.F., Grigorieff,N. and Korostelev,A.A. (2016) Ribosome*RelA structures reveal the mechanism of stringent response activation. *Elife*, **5**, e17029.
8. Battesti,A. and Bouveret,E. (2006) Acyl carrier protein/SpoT interaction, the switch linking SpoT-dependent stress response to fatty acid metabolism. *Mol. Microbiol.*, **62**, 1048–1063.
9. Atkinson,G.C., Tenson,T. and Hauryliuk,V. (2011) The RelA/SpoT homolog (RSH) superfamily: distribution and functional evolution of ppGpp synthetases and hydrolases across the tree of life. *PLoS One*, **6**, e23479.
10. Boutte,C.C. and Crosson,S. (2011) The complex logic of stringent response regulation in Caulobacter crescentus: starvation signalling in an oligotrophic environment. *Mol. Microbiol.*, **80**, 695–714.
11. Lesley,J.A. and Shapiro,L. (2008) SpoT regulates DnaA stability and initiation of DNA replication in carbon-starved Caulobacter crescentus. *J. Bacteriol.*, **190**, 6867–6880.
12. Curtis,P.D. and Brun,Y.V. (2010) Getting in the loop: regulation of development in Caulobacter crescentus. *Microbiol. Mol. Biol. Rev.*, **74**, 13–41.
13. Chiaverotti,T.A., Parker,G., Gallant,J. and Agabian,N. (1981) Conditions that trigger guanosine tetraphosphate accumulation in Caulobacter crescentus. *J. Bacteriol.*, **145**, 1463–1465.
14. Gonzalez,D. and Collier,J. (2014) Effects of (p)ppGpp on the progression of the cell cycle of Caulobacter crescentus. *J. Bacteriol.*, **196**, 2514–2525.
15. Ronneau,S., Petit,K., De Bolle,X. and Hallez,R. (2016) Phosphotransferase-dependent accumulation of (p)ppGpp in response to glutamine deprivation in Caulobacter crescentus. *Nat. Commun.*, **7**, 11423.
16. Krol,E. and Becker,A. (2011) ppGpp in Sinorhizobium meliloti: biosynthesis in response to sudden nutritional downshifts and modulation of the transcriptome. *Mol. Microbiol.*, **81**, 1233–1254.
17. Wells,D.H. and Long,S.R. (2002) The Sinorhizobium meliloti stringent response affects multiple aspects of symbiosis. *Mol. Microbiol.*, **43**, 1115–1127.
18. Casadaban,M.J. and Cohen,S.N. (1980) Analysis of gene control signals by DNA fusion and cloning in Escherichia coli. *J. Mol. Biol.*, **138**, 179–207.
19. Mendrygal,K.E. and Gonzalez,J.E. (2000) Environmental regulation of exopolysaccharide production in Sinorhizobium meliloti. *J. Bacteriol.*, **182**, 599–606.
20. Beaufay,F., Coppine,J., Mayard,A., Laloux,G., De Bolle,X. and Hallez,R. (2015) A NAD-dependent glutamate dehydrogenase coordinates metabolism with cell division in Caulobacter crescentus. *EMBO J.*, **34**, 1786–1800.
21. Boutte,C.C., Henry,J.T. and Crosson,S. (2012) ppGpp and polyphosphate modulate cell cycle progression in Caulobacter crescentus. *J. Bacteriol.*, **194**, 28–35.
22. Bahr,T., Luttmann,D., Marz,W., Rak,B. and Gorke,B. (2011) Insight into bacterial phosphotransferase system-mediated signaling by interspecies transplantation of a transcriptional regulator. *J. Bacteriol.*, **193**, 2013–2026.
23. Wang,G., Peterkofsky,A., Keifer,P.A. and Li,X. (2005) NMR characterization of the Escherichia coli nitrogen regulatory protein IIANtr in solution and interaction with its partner protein, NPr. *Protein Sci.*, **14**, 1082–1090.
24. Lee,C.R., Park,Y.H., Kim,M., Kim,Y.R., Park,S., Peterkofsky,A. and Seok,Y.J. (2013) Reciprocal regulation of the autophosphorylation of enzyme INtr by glutamine and alpha-ketoglutarate in Escherichia coli. *Mol. Microbiol.*, **88**, 473–485.
25. Goodwin,R.A. and Gage,D.J. (2014) Biochemical characterization of a nitrogen-type phosphotransferase system reveals that enzyme EI(Ntr) integrates carbon and nitrogen signaling in Sinorhizobium meliloti. *J. Bacteriol.*, **196**, 1901–1907.

26. De Nisco,N.J., Abo,R.P., Wu,C.M., Penterman,J. and Walker,G.C. (2014) Global analysis of cell cycle gene expression of the legume symbiont Sinorhizobium meliloti. *Proc. Natl. Acad. Sci. U.S.A.*, **111**, 3217–3224.
27. Gentry,D.R. and Cashel,M. (1996) Mutational analysis of the Escherichia coli spoT gene identifies distinct but overlapping regions involved in ppGpp synthesis and degradation. *Mol. Microbiol.*, **19**, 1373–1384.
28. Mechold,U., Murphy,H., Brown,L. and Cashel,M. (2002) Intramolecular regulation of the opposing (p)ppGpp catalytic activities of Rel(Seq), the Rel/Spo enzyme from Streptococcus equisimilis. *J. Bacteriol.*, **184**, 2878–2888.
29. Gropp,M., Strausz,Y., Gross,M. and Glaser,G. (2001) Regulation of Escherichia coli RelA requires oligomerization of the C-terminal domain. *J. Bacteriol.*, **183**, 570–579.
30. Jain,V., Saleem-Batcha,R., China,A. and Chatterji,D. (2006) Molecular dissection of the mycobacterial stringent response protein Rel. *Protein Sci.*, **15**, 1449–1464.
31. Singal,B., Balakrishna,A.M., Nartey,W., Manimekalai,M.S.S., Jeyakanthan,J. and Gruber,G. (2017) Crystallographic and solution structure of the N-terminal domain of the Rel protein from Mycobacterium tuberculosis. *FEBS Lett.*, **591**, 2323–2337.
32. Grant,G.A. (2006) The ACT domain: a small molecule binding domain and its role as a common regulatory element. *J. Biol. Chem.*, **281**, 33825–33829.
33. Fang,M. and Bauer,C.E. (2018) Regulation of stringent factor by branched-chain amino acids. *Proc. Natl. Acad. Sci. U.S.A.*, **115**, 6446–6451.
34. Lee,J.W., Park,Y.H. and Seok,Y.J. (2018) Rsd balances (p)ppGpp level by stimulating the hydrolase activity of SpoT during carbon source downshift in Escherichia coli. *Proc. Natl. Acad. Sci. U.S.A.*, **115**, E6845–E6854.
35. Park,Y.H., Lee,C.R., Choe,M. and Seok,Y.J. (2013) HPr antagonizes the anti-sigma70 activity of Rsd in Escherichia coli. *Proc. Natl. Acad. Sci. U.S.A.*, **110**, 21142–21147.
36. Hallez,R., Bellefontaine,A.F., Letesson,J.J. and De Bolle,X. (2004) Morphological and functional asymmetry in alpha-proteobacteria. *Trends Microbiol.*, **12**, 361–365.
37. Karstens,K., Zschiedrich,C.P., Bowien,B., Stulke,J. and Gorke,B. (2014) Phosphotransferase protein EIIANtr interacts with SpoT, a key enzyme of the stringent response, in Ralstonia eutropha H16. *Microbiology*, **160**, 711–722.
38. Deghelt,M., Mullier,C., Sternon,J.F., Francis,N., Laloux,G., Dotreppe,D., Van der Henst,C., Jacobs-Wagner,C., Letesson,J.J. and De Bolle,X. (2014) G1-arrested newborn cells are the predominant infectious form of the pathogen Brucella abortus. *Nat. Commun.*, **5**, 4366.